# Depositional Characteristics of Metal Coating on Single-Crystal $TiO_2$ Nanowires

**Baomei Wen,[†,‡] Chunyan Liu,*[,†] and Yun Liu[†]**

*Technical Institute of Physics and Chemistry, Chinese Academy of Sciences, Beijing 100101, China, and Graduate School of the Chinese Academy of Sciences, Beijing 100101, China*

*Received: February 22, 2005; In Final Form: April 14, 2005*

Ultralong single-crystalline $TiO_2$ nanowires were prepared by a simple, low-cost solvothermal process. Silver nitrate, neodymium chloride, ceric nitrate, stannic chloride hydrate, and cadmium chloride were used as metal sources and deposited by reduction on the surface of $TiO_2$ nanowires. The composites were subsequently characterized by transmission electron microscopy, and their coverage was compared. The nature of the coatings on the $TiO_2$ nanowires varies from metal to metal. A novel approach on modified one-dimensional nanostructures with metal coating was developed, which has great potential applications in catalysts, sensors, and nanoscale devices.

## Introduction

Over the past decade, low-dimensional nanostructures have attracted growing interest due to their peculiar, fascinating properties, as well as their unique applications complementary to the bulk materials. One-dimensional nanostructures, such as nanotubes[1−3] and nanowires,[4−8] represent a particularly attractive class of nanostructures because they can function as both nanoscale device elements and interconnects, retaining unique properties due to size confinement in the radial direction. Nanowires, in particular, play an important role as both interconnects and active components in fabricating nanoscale electronic and photonic devices. Until very recently, the advance in the utilization of nanowires had been relatively slow, probably due to difficulties associated with the synthesis of such nanostructures with well-controlled size, phase purity, crystallinity, and chemical composition.

Controlling the size of nanowires can bring about changes in some of their properties, while metal-modified nanowires will provide a far more favorable approach to modulate their properties. Oxide-supported metal is of great interest because the structural, chemical, and electronic properties of the metal oxide interface directly affect the optimum utilization of transition metal catalysts, ceramics, and photovoltaic devices.[9−11] The multicomponent systems, such as a (nanoscale) core of one material coated with a (nanoscale) shell of other materials, are referred to as core−shell nanostructures. The major goal of preparing nanocomposites with core−shell structures is to improve catalytic, sensing, or material luminescent properties. At present, many methods have been developed to achieve this requirement. Therein, chemical reduction has been most popularly used in the literature.[12−14] In addition, vapor deposition,[15] calcination treatment,[16] electrochemical method,[17] and photodeposition[13,14] have also been used to prepare core−shell structures. However, we note that many research works have focused on spherical core−shell systems, with little attention paid to one-dimensional (i.e., nanowire) core−shell structures.

Among the various materials, the well-known $TiO_2$ and metal can still offer unexplored opportunities for the realization of novel nanocomposite systems. $TiO_2$ is one of the most investigated oxide materials owing to its important role in applications related to environmental cleaning and protection,[18] photocatalysis,[19] gas sensing,[20] and fabrication of solar cells and batteries.[21] In this paper, we develop a simple solvothermal method and successfully synthesize ultralong single-crystalline anatase $TiO_2$ nanowires with lengths of up to a few millimeters. Subsequently, with the use of titania as an oxide support, we achieve various metal-coated $TiO_2$ nanowire core−shell structures, and primarily explore the novel nanostructures in fundamental studies.

## Experimental Section

**Chemical Reagents.** All chemicals were used as received without further purification. Degussa P25 powders (average particle size 30 nm and specific surface area of 50 $m^2 \cdot g^{-1}$), sodium hydroxide (NaOH, AR), ethanol ($C_2H_5OH$, AR), silver nitrate ($AgNO_3$, AR), neodymium chloride ($NdCl_3 \cdot 6H_2O$, AR), ceric nitrate ($Ce(NO_3) \cdot 6H_2O$, AR), stannic chloride hydrate ($SnCl_4 \cdot 5H_2O$, AR), and cadmium chloride ($CdCl_2 \cdot 2.5H_2O$, AR) were purchased from Beijing Chemical Factory. Doubly distilled deionized water was used during all the experiments.

**Preparation of $TiO_2$ Nanowires.** The synthesis of $TiO_2$ nanowires was described particularly in our previous work.[22] In a typical method, 0.5 g of commercial Degussa P25 powder was mixed with NaOH aqueous solution of 10 M and absolute ethanol; the volume ratio of NaOH aqueous solution to ethanol was 1:1. Then 20 mL of the mixed solution was transferred into a Teflon-lined stainless steel autoclave of 100 mL capacity. The autoclave was maintained at 170−200 °C under autogenous pressure for 24 h and then cooled to room temperature naturally. The obtained sample was filtered, washed with dilute HCl aqueous solution and deionized water several times until the pH value of the washing solution was about 7.0, and dried at 60 °C for 6 h in air.

**Preparation of Composite Materials.** For the preparation of various composites, a certain amount of $TiO_2$ nanowires was dispersed in 10 mL of deionized water via sonication; 5 mL of absolute ethanol was subsequently added. The pH of the solution

* Corresponding author. E-mail: cyliu@mail.ipc.ac.cn.
† Technical Institute of Physics and Chemistry.
‡ Graduate School of the Chinese Academy of Sciences.

10.1021/jp050934f CCC: $30.25 
Published on Web 06/04/2005

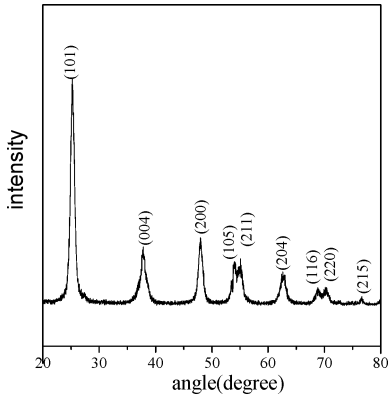


**Figure 1.** XRD pattern of $TiO_2$ nanowires.

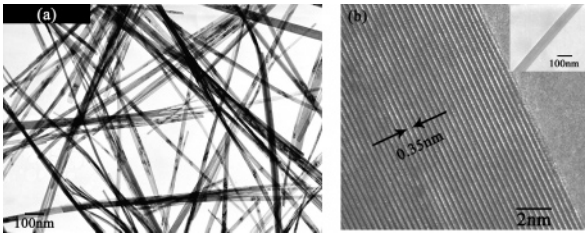


**Figure 2.** TEM images of $TiO_2$ nanowires. (a) Low magnification; (b) high magnification. The inset is an individual nanowire.

was adjusted to be slightly basic with NaOH of 1 mol $mL^{-1}$. After stirring for 30 min, a metal source was added. The reducing reaction was kept at 50 °C for 8 h. The product obtained was filtered, washed three times with deionized water and alcohol, and then dried at 60 °C for 6 h in air.

**Characterization of Composite Materials.** The composite materials were characterized by X-ray powder diffraction (XRD) using a Rigaku DMAX-2000 X-ray diffractometer with Cu Kα radiation ($\lambda = 1.540\,56$ Å) at a scanning rate of 0.02° $s^{-1}$ in $2\theta$ ranging from 20° to 80° and images of transmission electron microscopy (TEM) recorded on a JEOL JEM-CX200 microscope at an acceleration voltage of 160 kV. The TEM samples were prepared by dropping an alcohol suspension of sample powders on a Formvar coated copper grid and letting the alcohol evaporate at room temperature. The high-resolution TEM (HRTEM) images were carried out on a Philips CM200/FEG microscope at an acceleration voltage of 200 kV. Energy-dispersive X-ray spectroscopy (EDX) was performed using nanoprobe mode on the JEOL scanning electron microscope. Infrared (IR) spectra were obtained on a Bio-Rad FTS165 spectrometer. UV−vis spectra were measured in a diffuse reflectance mode on a Varian DMS 300 spectrometer.

## Results and Discussion

Figure 1 shows the X-ray diffraction (XRD) pattern of the synthesized $TiO_2$ nanowires. All of the peaks can be readily indexed to the pure anatase phase with lattice constants $a = 3.7806$ Å and $c = 9.4977$ Å, which are basically in agreement with the reported values (JCPDS No. 21-1272). No characteristic peaks of other impurities are observed, which indicates that the product is of high purity.

Figure 2a shows a TEM image of the synthesized $TiO_2$ nanowires. It reveals that the products have a wirelike morphology with diameters of 20−80 nm, with lengths of up to a few millimeters, and the geometry of the nanowires is quite uniform.

Figure 2b shows a typical HRTEM image of a nanowire with a well-defined structure (the inset in Figure 2b). The fringes parallel to the nanowire axis correspond to an interplanar distance of about 0.35 nm. This fringe spacing is characteristic of the anatase crystal phase in the (101) plane. The clear lattice fringes indicate that the nanowires are single crystalline and the structure is perfect.

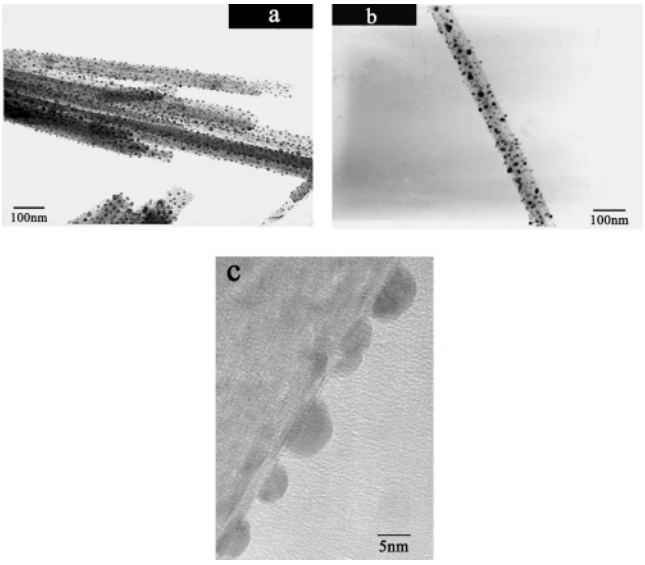


**Figure 3.** TEM images of Ag-coated $TiO_2$ nanowires. (a) Low magnification; (b) typical individual Ag-coated $TiO_2$ nanowire; (c) local high-resolution image.

The morphology of deposition of various metals on the $TiO_2$ nanowires shows much variation. Representatively, the TEM images of Ag-coated $TiO_2$ nanowires are shown in Figure 3. From these images, it can be seen that the coverage of silver is nearly uniform over the entire length of the nanowires. A local HRTEM image in Figure 3c indicates that Ag particles are spherelike and the size is about 3−8 nm. The EDX spectrum is presented in Figure 5a, which clearly confirms the presence of Ag, along with Ti, O, and other expected elements.

More metal coverage, such as Nd, Ce, Cd, and Sn, is studied, illustrated in parts a, b, c, and d, respectively, of Figure 4. The coverage shows different morphological natures. The coating of metal Nd on the $TiO_2$ nanowires reveals properties similar to that of metal Ag. A homogeneous coverage is obtained over the entire length of the nanowires (Figure 4a). It is noteworthy, however, that metal Nd on the $TiO_2$ nanowires shows regular rectangular shapes (as shown in Figure 4e). Moreover, the deposition of metal Nd on the $TiO_2$ nanowires has a fixed direction, with the rectangular Nd particles deposited along the $TiO_2$ nanowire axis. Also, the rectangular Nd particles show a monodispersed coating nature on the $TiO_2$ nanowires. The EDX spectrum further confirms the presence of Nd element (Figure 5b).

The deposition of metal Ce on the $TiO_2$ nanowires is quite inhomogeneous. Many aggregates of nanometer-sized clusters cover the $TiO_2$ nanowires as shown in Figure 4b,f. The Cd coverage seems more difficult. Only a few clusters cover on the $TiO_2$ nanowires with much separated segregation observed (Figure 4c). For metal Sn (Figure 4d), we obtain a more homogeneous coverage than with either metal Ce or Cd.

The morphology of deposited metal clusters is affected by many factors, such as the substrate temperature, the thermal stability of the clusters upon high-temperature annealing, and the surface defects of the substrate.[23,24] Bauer proposed three growth modes on the formation of the metal islands and films (particle size within nanoscale) on a substrate: the Frank−Van der Merwe (monolayer by monolayer FM growth) mode; the Stranski−Krastanov (layer growth up to one or a few monolayer

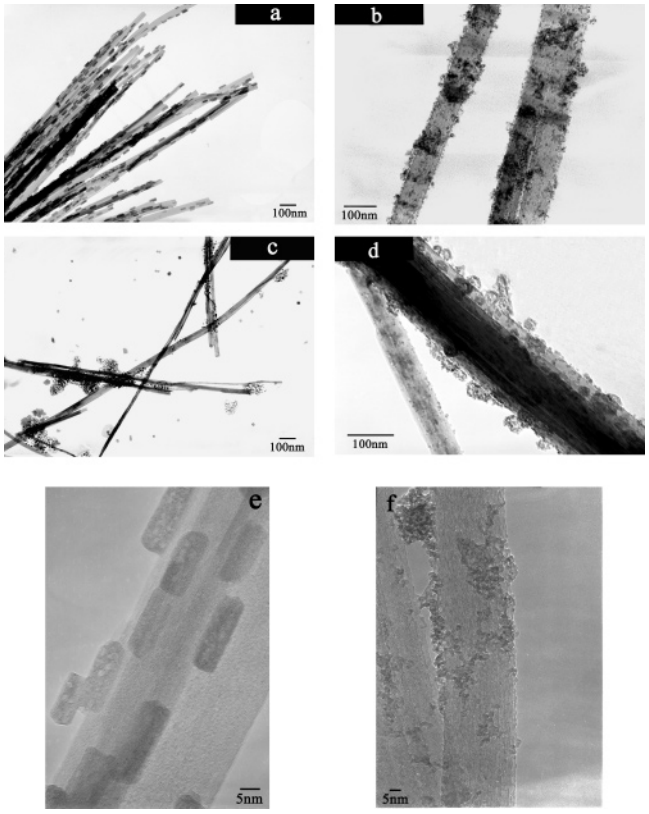


**Figure 4.** TEM images of $TiO_2$ nanowires coated with various metals. (a) Nd; (b) Ce; (c) Cd; (d) Sn; (e) HRTEM image of Nd-coated sample; (f) HRTEM image of Ce-coated sample.

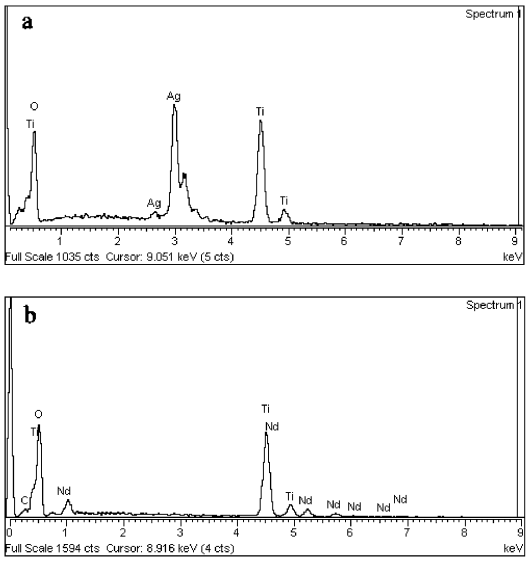


**Figure 5.** EDX spectra of Ag- and Nd-coated $TiO_2$ nanowires.

plus crystallites, SK growth) mode; and the Volmer−Weber (three-dimensional crystallites without a preceding adsorbed layer, VW growth) mode.[25] A simple explanation of the different growth modes can be formulated in terms of surface energy criteria. If the condensate has a surface energy $\gamma_A$, substrate $\gamma_S$, and the interface between the two $\gamma_I$, then the condition $\gamma_A + \gamma_I < \gamma_S$ will favor the covering over of the substrate by spreading of the condensate (wetting or FM mode), while $\gamma_A + \gamma_I > \gamma_S$ will favor nonwetting (SK or VW mode). Subsequently, Argile[26] put forward the two additional growth modes that were referred as "simultaneous multilayer" growth (SM) and "monolayer plus simultaneous multilayer" growth (MSM).

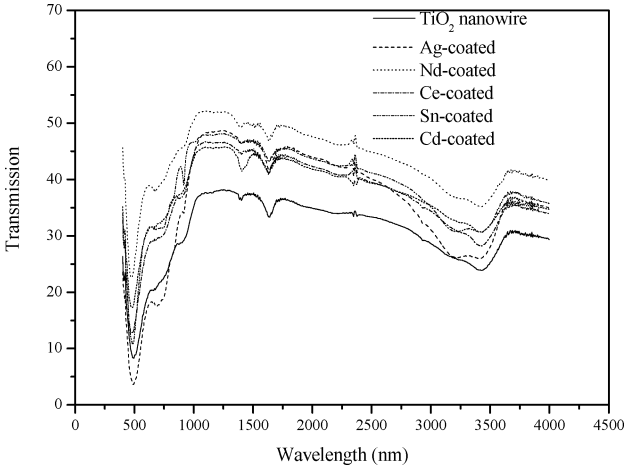


**Figure 6.** FT-IR spectra of various metal-coated $TiO_2$ nanowires.

Obviously, in our experiments, different metal coatings grow according to different modes. The growth of Ag and Nd coating follows the VW mode. Ce and Cd coatings grow according to the SM mode, while Sn coating grows according to the MSM mode.

From a surface science viewpoint, a more general interpretation of the growth for supported metal clusters is as follows. Initially, the metal is deposited as a single isolated atom. Then, at low coverage, isolated metal atoms coalesce into two-dimensional islands, which may appear flat or raftlike. Three-dimensional crystallites are formed by increasing the metal loading or support temperature. Meanwhile, the shape of metal clusters is related to the strength of the metal−support interaction. It is inferred that when the metal−metal bonds are stronger than the metal−substrate bonds, three-dimensional cluster formation (i.e., Ag and Nd coating) is preferred to two-dimensional coverage of the surface (i.e., the first layer of Sn coating).

The coating layers can affect the surface state of $TiO_2$ nanowires. FT-IR transmittance spectra (KBr pellets method) of the samples are measured to investigate structural information of $TiO_2$ nanowires and hydroxyl groups on the wire surface. The FT-IR spectrum of the coating samples is shown in Figure 6. A sharp absorption band at 500−520 $cm^{-1}$ and a sharp, weak peak at 700 $cm^{-1}$ can be assigned to $\delta$(Ti−O, metal−O). The broad, strong peaks at 3400 and 1640 $cm^{-1}$ show the characteristic absorption of $\delta$(−OH) and $\delta$(−O−H) function groups, which are due to Ti−OH and the hydrated species.[27] Notably, compared to a IR spectrum of the as-prepared $TiO_2$ nanowires, the absorption bands of all coating samples at 3400 $cm^{-1}$ are broader and shift to shorter wavenumbers due to the influence of the coverage on hydroxyl groups of the nanowire surface. The increasing intensity of the peak at 700 $cm^{-1}$ can be considered a result of the stronger interaction of metal and oxygen. Obviously, the metal coating changes the hydrophilic property of the $TiO_2$ surface.

Surface plasmon absorption is a very important characteristic of metallic nanoparticles, from which metallic nanoparticles find application in optical electronics, linear and nonlinear optics, and so on. Actually, plasmon absorption is very sensitive to the changes in the surrounding medium, such that the changes in absorption can provide useful information on the interaction between metal clusters and the support.[28]

We carried out UV−visible diffuse reflectance spectroscopy to further investigate the structural information of the coating samples. The UV−vis spectra of the coating samples are shown

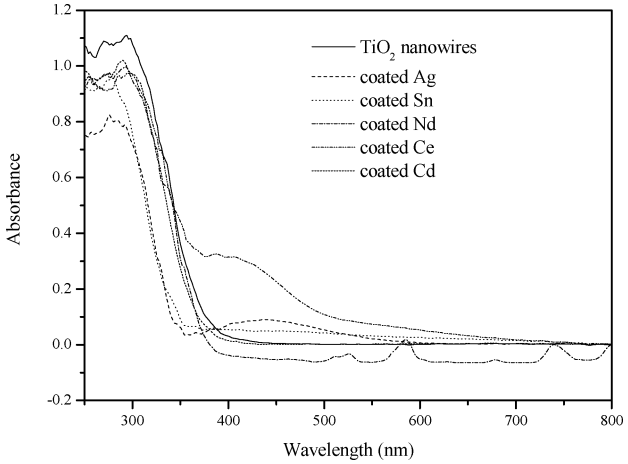


**Figure 7.** UV−vis apectra of neat and metal-coated $TiO_2$ nanowires.

**TABLE 1: Band Gap Energies of Neat and Metal-Coated $TiO_2$ Nanowires**

| sample | band gap energy (eV) |
|---|---|
| neat | 3.10 |
| Ag coated | 3.45 |
| Sn coated | 3.33 |
| Nd coated | 3.28 |
| Ce coated | 2.62 |
| Cd coated | 3.15 |

in Figure 7. A broad band at 480 nm is attributed to the surface plasmon resonance of metallic silver nanoparticles,[29] which appears on the UV−vis absorption spectrum of silver-coated $TiO_2$ nanowires. Compared to as-prepared $TiO_2$ nanowires, the absorption edge of the Ag-coated sample was shifted to a shorter wavelength, which corresponds to a high band gap energy. Through plotting $(\alpha)^{1/2}$ versus $hc/\lambda$ (where $\alpha$ is the absorption coefficient, $h$ is Planck's constant, $c$ is the velocity of light, and $\lambda$ is wavelength), we calculate that the band gap energies increase from 3.10 eV in the noncoated samples to 3.45 eV after coating with Ag. Table 1 lists the band gap energies of the samples coated with various metals, which accord with the results of Figure 7. Compared to as-prepared $TiO_2$ nanowires, the absorption of the Ce-coated sample extended to 400−500 nm, showing a large red shift. In the Nd-coated sample, absorption bands with shoulders in the visible light region were observed. However, in other coating samples, the absorption edges seem a little blue shifted (Figure 7 and Table 1), to some extent, because of the surface deposition of metal clusters. Thus, it can be inferred that an interaction exists between the coated metals and $TiO_2$ nanowire. Accordingly, it can also be inferred that the behavior of photocatalysts can possibly be changed, making it convenient to study the effect of metal coating materials on the photocatalytic performance of $TiO_2$ nanowires.

## Conclusions

We have investigated the deposition of various metals on ultralong single-crystalline $TiO_2$ nanowires. It is found that various metals have different coating natures and morphologies on the $TiO_2$ nanowires.

One-dimensional nanostructures provide a better model system for investigating the dependence of electronic transport, optical properties, and mechanical properties on size confinement and dimensionality. This represents an extension of modified nanostructures used in spherical core−shell systems to one-dimensional core−shell structures, widening the range of possible applications for nanowires.

**Acknowledgment.** This work was supported by the 863 Projects of China and the National Natural Science Foundation of China (90306003, 90406024).

## References and Notes

(1) Hu, J.; Odom, T. W.; Lieber, C. M. *Acc. Chem. Res.* **1999**, *32*, 435.

(2) Bockrath, M.; Liang, W. J.; Bozovic, D.; Hafner, J. H.; Lieber, C. M.; Tinkham, M.; Park, H. K. *Science* **2001**, *291*, 283.

(3) Liang, W. J.; Bockrath, M.; Bozovic, D.; Hafner, J. H.; Tinkham, M.; Park, H. *Nature* **2001**, *411*, 665.

(4) Morales, A. M.; Lieber, C. M. *Science* **1998**, *279*, 208.

(5) Holmes, J. D.; Johnston, K. P.; Doty, R. C.; Korgel, B. A. *Science* **2000**, *287*, 1471.

(6) Cui, Y.; Lieber, C. M. *Science* **2001**, *291*, 851.

(7) Duan, X.; Huang, Y.; Cui, Y.; Wang, J.; Lieber, C. M. *Nature* **2001**, *409*, 66.

(8) Huang, M. H.; Mao, S.; Feick, H.; Yan, H. Q.; Wu, Y. Y.; Kind, H.; Weber, E.; Russo, R.; Yang, P. D. *Science* **2001**, *292*, 1879.

(9) Campbell, C. T. *Surf. Sci. Rep.* **1997**, *27*, 1.

(10) Goodman, D. W. *Surf. Rev. Lett.* **1995**, *2*, 9.

(11) Diebold, U.; Pan, J. M.; Madey, T. E. *Surf. Sci.* **1995**, *331*, 845.

(12) Chandrasekharan, N.; Kamat, P. V. *J. Phys. Chem. B* **2000**, *104*, 10851.

(13) Dawson, A.; Kamat, P. V. *J. Phys. Chem. B* **2001**, *105*, 960.

(14) Subramanian, V.; Wolf, E. E.; Kamat, P. V. *Langmuir* **2003**, *19*, 469.

(15) Rodriguez, J. A.; Liu, G.; Jirsak, T.; Hrbek, J.; Chang, Z.; Dvorak, J.; Maiti, A. *J. Am. Chem. Soc.* **2002**, *124*, 5242.

(16) Zanella, R.; Giorgio, S.; Henry, C. R.; Louis, C. *J. Phys. Chem. B* **2002**, *106*, 7634.

(17) Liu, Y. C.; Juang, L. C. *Langmuir* **2004**, *20*, 6951.

(18) Andersson, M.; Osterlund, L.; Ljungstrom, S.; Palmqvist, A. *J. Phys. Chem. B* **2002**, *414*, 338.

(19) Tada, H.; Suzuki, F.; Ito, S.; Akita, T.; Tanaka, K.; Kawahara, T.; Kobayashi, H. *J. Phys. Chem. B* **2002**, *106*, 8714.

(20) Rothschild, A.; Levakov, A.; Shapira, Y.; Ashkenasy, N.; Komem, Y. *Surf. Sci.* **2003**, *456*, 532.

(21) Gratzel, M. *Nature* **2001**, *414*, 338.

(22) Wen, B.; Liu, C.; Liu, Y. Solvothermal synthesis of ultralong single-crystalline $TiO_2$ nanowires. *New J. Chem.*, in press.

(23) Schaffner, M. H.; Patthey, F.; Schneider, W. D. *Surf. Sci.* **1998**, *417*, 159.

(24) Zhang, L.; Cosandey, F.; Persaud, R.; Madey, T. E. *Surf. Sci.* **1999**, *439*, 73.

(25) Bauer, E. *Z. Kristallogr.* **1958**, *110*, 372.

(26) Argile, C.; Rhead, G. E. *Surf. Sci. Rep.* **1989**, *10*, 277.

(27) Yasumori, A.; Shinoda, H.; Kameshima, Y.; Hayashi, S. *J. Mater. Chem.* **2001**, *11*, 1253.

(28) Mie, G. *Ann. Phys.* **1908**, *25*, 377.

(29) He, J. H.; Ichinose, I.; Fujikawa, S.; Kunitake, T.; Nakao, A. *Chem. Commun.* **2002**, 1910.